

Spectroscopic Properties of Sm^{3+} Doped in Lead Lithium Bismuth Silicate Glasses

S. L. MEENA

Ceremic Laboratory, Department of Physics, Jai Narain Vyas University, Jodhpur 342001(Raj.) India

*Corresponding Author E-Mail: shankardiya7@rediffmail.com

Received: 05.09.2018

Accepted: 13.10.2018

Published Online 15.10.2018

<https://doi.org/10.30731/ijcps.7.5.2018.1-10>

Abstract

Glass sample of Lead Lithium Bismuth Silicate $(60-x) \text{Bi}_2\text{O}_3:10\text{PbO}:10\text{Li}_2\text{O}:20\text{SiO}_2: x \text{Sm}_2\text{O}_3$ (where $x=1,1.5,2$ mol%) have been prepared by melt-quenching technique. The amorphous nature of the prepared glass samples was confirmed by X-ray diffraction. The absorption spectra of three Sm^{3+} doped lead lithium bismuth silicate glasses have been recorded at room temperature. The various interaction parameters like Slater-Condon parameters F_k ($k=2,4,6$), Lande parameters (ζ_{4f}), nephelauxetic ratio (β'), bonding parameters ($b^{1/2}$) and Racah parameters E^k ($k=1,2,3$) have been computed. Judd-Ofelt intensity parameters and laser parameters have also been calculated.

Keywords: Lead lithium bismuth silicate glasses, Energy interaction parameters, Optical properties, Judd-Ofelt analysis.

Introduction:

Rare earth doped transparent bismuth silicate glasses and glass ceramics are of increasing interests in various optical applications, because of their superior optical properties, such as high refractive index, high density and high reflection losses [1-5]. Consequently the properties of glass of the system lead lithium bismuth silicate have attracted much interest [6-9].

Recently, many rare earth ions-doped glasses found important in the area of solid state lasers, fiber laser, wave guide laser, laser amplifier in optical communication and optical data storage [10-13]. The stimulated emission cross-section (σ_p) parameter is the most important parameter. Its value signifies the rate of energy extraction from the laser material and is generally used to predict laser action in different rare earth doped glass specimens.

The aim of the present study is to prepare the Sm^{3+} doped Lead lithium bismuth silicate glass with different Sm_2O_3 concentrations. The absorption spectra, fluorescence spectra of Sm^{3+} of the glasses were investigated. The Judd-Ofelt theory has been applied to compute the intensity parameters Ω_λ ($\lambda=2, 4, 6$). These intensity parameter have been used to evaluate optical properties such as spontaneous emission probability, branching ratio, radiative life time and stimulated emission cross section.

Experimental Techniques:

Preparation of glasses

The following Sm³⁺ doped bismuth silicate glass samples (60-x) Bi₂O₃:10PbO:10Li₂O:20SiO₂: x Sm₂O₃. (where x=1,1.5, 2) have been prepared by melt-quenching method. Analytical reagent grade chemical used in the present study consist of Bi₂O₃, PbO, Li₂O, SiO₂ and Sm₂O₃. They were thoroughly mixed by using an agate pestle mortar. then melted at 1460⁰C by an electrical muffle furnace for 2h., After complete melting, the melts were quickly poured in to a preheated stainless steel mould and annealed at temperature of 390⁰C for 2h to remove thermal strains and stresses. Every time fine powder of cerium oxide was used for polishing the samples. The glass samples so prepared were of good optical quality and were transparent. The chemical compositions of the glasses with the name of samples are summarized in Table 1.

Table 1

Chemical composition of the glasses

Sample	Glass composition (mol %)
LLBS (UD)	60 Bi ₂ O ₃ :10PbO:10Li ₂ O:20SiO ₂
LLBS (SM1)	59 Bi ₂ O ₃ :10PbO:10Li ₂ O:20SiO ₂ : 1 Sm ₂ O ₃
LLBS (SM 1.5)	58.5 Bi ₂ O ₃ :10PbO:10Li ₂ O:20SiO ₂ : 1.5 Sm ₂ O ₃
LLBS (SM 2)	58 Bi ₂ O ₃ :10PbO:10Li ₂ O:20SiO ₂ 2 Sm ₂ O ₃
LLBS (UD)	-Represents undoped Lead Lithium Bismuth Silicate glass specimens
LLBS (SM)	-Represents Sm ³⁺ doped Lead Lithium Bismuth Silicate glass specimens

Theory

Oscillator Strength

The intensity of spectral lines is expressed in terms of oscillator strengths using the relation [14].

$$f_{\text{expt.}} = 4.318 \times 10^{-9} \int \epsilon(\nu) d\nu \quad (1)$$

where, $\epsilon(\nu)$ is molar absorption coefficient at a given energy ν (cm⁻¹), to be evaluated from Beer–Lambert law.

Under Gaussian Approximation, using Beer–Lambert law, the observed oscillator strengths of the absorption bands have been experimentally calculated [15], using the modified relation:

$$P_m = 4.6 \times 10^{-9} \times \frac{1}{cl} \log \frac{I_0}{I} \times \Delta\nu_{1/2} \quad (2)$$

where c is the molar concentration of the absorbing ion per unit volume, I is the optical path length, $\log I_0/I$ is optical density and $\Delta\nu_{1/2}$ is half band width.

Judd-Ofelt Intensity Parameters

According to Judd [16] and Ofelt [17] theory, independently derived expression for the oscillator strength of the induced forced electric dipole transitions between an initial J manifold $|4f^N(S, L) J\rangle$ level and the terminal J' manifold $|4f^N(S', L') J'\rangle$ is given by:

$$\frac{8\pi^2 mc \bar{\nu}}{3h(2J+1)n} \frac{1}{n} \left[\frac{(n^2+2)^2}{9} \right] \times S(J, J') \quad (3)$$

Where, the line strength S (J, J') is given by the equation

$$S(J, J') = e^2 \sum_{\lambda=2, 4, 6} \Omega_{\lambda} \langle 4f^N(S, L) J \| U^{(\lambda)} \| 4f^N(S', L') J' \rangle^2$$

In the above equation m is the mass of an electron, c is the velocity of light, $\bar{\nu}$ is the wave number of the transition, h is Planck's constant, n is the refractive index, J and J' are the total angular momentum of the initial and final level respectively, Ω_{λ} ($\lambda = 2, 4, 6$) are known as Judd-Ofelt intensity parameters .

Radiative Properties

The Ω_{λ} parameters obtained using the absorption spectral results have been used to predict radiative properties such as spontaneous emission probability (A) and radiative life time (τ_R), and laser parameters like fluorescence branching ratio (β_R) and stimulated emission cross section (σ_p).

The spontaneous emission probability from initial manifold $|4f^N(S', L') J'\rangle$ to a final manifold $|4f^N(S, L) J\rangle$ is given by:

$$A[(S', L') J'; (S, L) J] = \frac{64 \pi^2 \bar{\nu}^3}{3h(2J'+1)} \left[\frac{n(n^2+2)^2}{9} \right] \times S(J', J) \quad (4)$$

$$\text{Where, } S(J', J) = e^2 [\Omega_2 \| U^{(2)} \|^2 + \Omega_4 \| U^{(4)} \|^2 + \Omega_6 \| U^{(6)} \|^2]$$

The fluorescence branching ratio for the transitions originating from a specific initial manifold $|4f^N(S', L') J'\rangle$ to a final manifold $|4f^N(S, L) J\rangle$ is given by

$$\beta_R[(S', L') J'; (S, L) J] = \sum_{SLJ} \frac{A[(S', L') J'; (S, L) J]}{A[(S', L') J'; (S, L) J]} \quad (5)$$

where, the sum is over all terminal manifolds.

The radiative life time is given by

$$\tau_{rad} = \sum_{SLJ} A[(S', L') J'; (S, L) J] = A_{Total}^{-1} \quad (6)$$

Where, the sum is over all possible terminal manifolds. The stimulated emission cross -section for a transition from an initial manifold $|4f^N(S', L') J'\rangle$ to a final manifold

$|4f^N(S, L)J\rangle$ is expressed as

$$\sigma_p(\lambda_p) = \left[\frac{\lambda_p^4}{8\pi c n^2 \Delta\lambda_{eff}} \right] \times A[(S', L') J'; (\bar{S}, \bar{L}) \bar{J}] \quad (7)$$

where, λ_p the peak fluorescence wavelength of the emission band and $\Delta\lambda_{eff}$ is the effective fluorescence line width.

Nephelauxetic Ratio (β) and Bonding Parameter ($b^{1/2}$)

The nature of the R-O bond is known by the Nephelauxetic Ratio (β') and Bonding Parameters ($b^{1/2}$), which are computed by using following formulae [18, 19]. The Nephelauxetic Ratio is given by

$$\beta' = \frac{\nu_g}{\nu_a} \quad (8)$$

where, ν_a and ν_g refer to the energies of the corresponding transition in the glass and free ion, respectively. The values of bonding parameter ($b^{1/2}$) are given by

$$b^{1/2} = \left[\frac{1-\beta'}{2} \right]^{1/2} \quad (9)$$

Results and Discussion:

XRD Measurement

Figure 1 presents the XRD pattern of the sample contain - Bi_2O_3 which is show no sharp Bragg's peak, but only a broad diffuse hump around low angle region. This is the clear indication of amorphous nature within the resolution limit of XRD instrument.

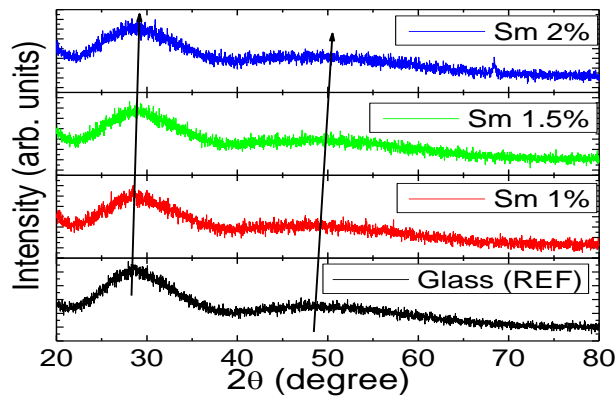


Fig. 1: X-ray diffraction pattern of Bi_2O_3 ; Li_2O ; PbO ; Si_2O_3 ; Sm_2O_3

Scanning electron microscopy (SEM)

SEM image explores the smooth surface of the sample. This smooth surface indicates that the amorphous behavior of the glass matrix and also we cannot identified any grain boundaries from the surface morphological image of the host LLBS glass sample as shown in Fig. 2

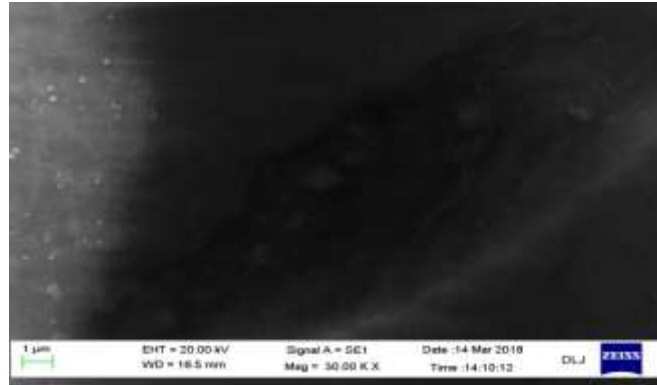


Fig.2 Scanning Electron Microscopy

Thermal Properties

Figure 3 shows the thermal properties of LLBS glass from 300°C to 1000°C. From the DSC curve of present glasses system, we can find out that no crystallization peak is apparent and the glass transition temperature T_g are 351°C, 450°C and 581°C respectively. The T_g increase with the contents of Sm_2O_3 increase. We could conclude that thermal properties of the LLBS glass are good for fiber drawing from the analysis of DSC curve.

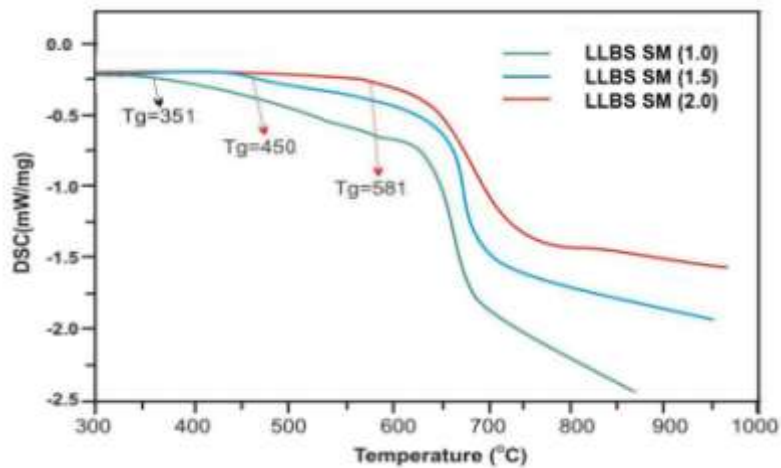


Fig.3: DSC curve of LLBS(SM) glasses.

Absorption Spectrum

The absorption spectra of Sm^{3+} doped LLBS (SM 01) glass specimen has been presented in Figure 4 in terms of optical density versus wavelength (nm). Ten absorption bands have been observed from the ground state $^6\text{H}_{5/2}$ to excited states $^6\text{F}_{1/2}$, $^6\text{F}_{7/2}$, $^6\text{F}_{9/2}$, $^4\text{G}_{7/2}$, $^4\text{I}_{9/2}$, $^4\text{M}_{7/2}$, $(^6\text{P}, ^4\text{P})_{5/2}$, $^4\text{F}_{7/2}$, $^4\text{D}_{1/2}$, and $(^4\text{D}, ^6\text{P})_{5/2}$ for Sm^{3+} doped LLBS glasses.

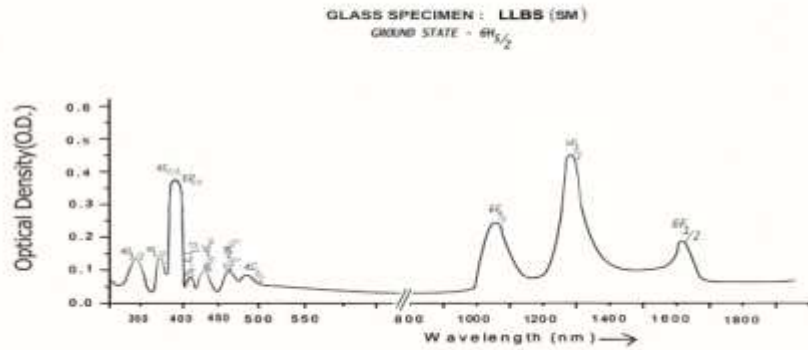


Fig.4: Absorption spectrum of Sm^{3+} doped LLBS glass

The experimental and calculated oscillator strengths for Sm^{3+} ions in Lead lithium bismuth silicate glasses are given in Table 2

Table 2: Measured and calculated oscillator strength ($P_m \times 10^{+6}$) of Sm^{3+} ions in LLBS glasses.

Energy level from ${}^6\text{H}_{5/2}$	Glass LLBS (SM01)		Glass LLBS (SM1.5)		Glass LLBS (SM02)	
	$P_{\text{exp.}}$	$P_{\text{cal.}}$	$P_{\text{exp.}}$	$P_{\text{cal.}}$	$P_{\text{exp.}}$	$P_{\text{cal.}}$
${}^6\text{F}_{1/2}$	1.56	1.62	1.55	1.61	1.53	1.60
${}^6\text{F}_{7/2}$	5.42	5.49	5.41	5.48	5.40	5.48
${}^6\text{F}_{9/2}$	3.77	3.83	3.74	3.81	3.73	3.81
${}^4\text{G}_{7/2}$	0.14	0.12	0.12	0.12	0.11	0.12
${}^4\text{I}_{9/2}, {}^4\text{M}_{15/2}, {}^4\text{I}_{11/2}$	1.12	1.87	1.11	1.87	1.09	1.86
${}^4\text{M}_{17/2}, {}^4\text{G}_{9/2}, {}^4\text{I}_{15/2}$	0.26	0.24	0.25	0.24	0.23	0.24
$({}^6\text{P}, {}^4\text{P})_{5/2}, {}^4\text{L}_{13/2}$	1.28	1.30	1.26	1.31	1.25	1.30
${}^4\text{F}_{7/2}, {}^6\text{P}_{3/2}, {}^4\text{K}_{11/2}$	5.52	5.61	5.51	5.62	5.49	5.62
${}^4\text{D}_{1/2}, {}^6\text{P}_{7/2}, {}^4\text{L}_{17/2}$	2.38	2.43	2.36	2.42	2.35	2.42
${}^4\text{D}_{3/2}, ({}^4\text{D}, {}^6\text{P})_{5/2}$	2.42	3.45	2.41	3.46	2.38	3.45
r.m.s. deviation	± 0.408		± 0.413		± 0.424	

Computed values of F_2 , Lande's parameter (ξ_{4f}), Nephelauxetic ratio (β') and bonding parameter ($b^{1/2}$) for Sm^{3+} doped LLBS glass specimen are given in Table 3.

Table 3: F_2 , ξ_{4f} , β' and $b^{1/2}$ parameters for Samarium doped glass specimen.

Glass Specimen	F_2	ξ_{4f}	β'	$b^{1/2}$
Sm^{3+}	358.82	1258.16	0.9337	0.1821

In the present case the three Ω_λ parameters follow the trend $\Omega_2 > \Omega_4 > \Omega_6$. The spectroscopic quality factor (Ω_4 / Ω_6) related with the rigidity of the glass system has been found to lie between 1.0948 and 1.1041 in the present glasses.

The value of Judd-Ofelt intensity parameters are given in **Table 4**

Table 4: Judd-Ofelt intensity parameters for Sm^{3+} doped LLBS glass specimens

Glass Specimen	$\Omega_2(\text{pm}^2)$	$\Omega_4(\text{pm}^2)$	$\Omega_6(\text{pm}^2)$	Ω_4 / Ω_6	Ref.
LLBS (SM01)	4.205	3.880	3.544	1.0948	P.W.
LLBS (SM1.5)	4.188	3.893	3.527	1.1038	P.W.
LLBS (SM02)	4.139	3.883	3.517	1.1041	P.W.
ZLBB(SM)	4.137	3.847	3.528	1.0904	[20]
YZLBB(SM)	4.080	3.810	3.517	1.0833	[21]

Fluorescence Spectrum

The fluorescence spectrum of Sm^{3+} doped in lead lithium bismuth silicate glass is shown in Figure 5. There are four bands observed in the Fluorescence spectrum of Sm^{3+} doped lead lithium bismuth silicate glass. The wavelengths of these bands along with their assignments are given in Table 5. Fig. (5).Shows the fluorescence spectrum with four peaks (${}^4G_{5/2} \rightarrow {}^6H_{5/2}$), (${}^4G_{5/2} \rightarrow {}^6H_{7/2}$), (${}^4G_{5/2} \rightarrow {}^6H_{9/2}$) and (${}^4G_{5/2} \rightarrow {}^6H_{11/2}$), respectively for glass specimens.

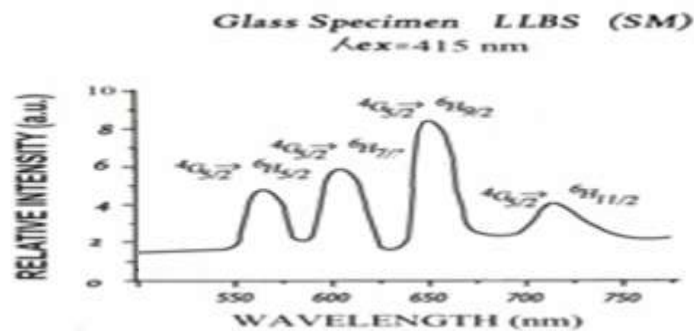


Fig.5: fluorescence spectrum of Sm^{3+} doped LLBS SM (01) glass

Conclusions:

In the present study, the glass samples of composition $(60-x) \text{Bi}_2\text{O}_3:10\text{PbO}:10\text{Li}_2\text{O}:20\text{SiO}_2: x \text{Sm}_2\text{O}_3$ (where $x=1,1.5, 2$) have been prepared by melt-quenching method. The spectroscopic quality factor (Ω_4 / Ω_6) related with the rigidity of the glass system has been found to lie between 1.0948 and 1.1041 in the present glasses.

The stimulated emission cross section (σ_p) has highest value for the transition (${}^4\text{G}_{5/2} \rightarrow {}^6\text{H}_{7/2}$) in all the glass specimens doped with Sm^{3+} ion. This shows that (${}^4\text{G}_{5/2} \rightarrow {}^6\text{H}_{7/2}$) transition is most probable transition.

References:

- [1] Reddy, R.R., Nazeer Ahmmed, Y. Abdul Azeem, P. Ramgopal, K. Rao, T.V.R., Buddhudu, S. and Sooraj Hussain, N. (2003). Absorption and emission spectral studies of Sm^{3+} and Dy^{3+} doped alkali fluoroborate glasses. *J. Quantum spectrosc. Radiat. Transfer.* 77: 149-63
- [2] Lakshminarayana, G., Qiu, J. (2009). Photoluminescence of Pr^{3+} , Sm^{3+} and $\text{Dy}^{3+}:\text{SiO}_2\text{-Al}_2\text{O}_3\text{-LiF-GdF}_3$ glass ceramics and Sm^{3+} , $\text{Dy}^{3+}:\text{GeO}_2\text{-B}_2\text{O}_3\text{-ZnO-LaF}_3$ Glasses. *Physica B*, 404: 1169-80.
- [3] Ahlawat, N., Singhi, S., Agarwal, A. and Bala, R. (2010). Influence of SiO_2 on the structure and optical properties of lithium bismuth silicate glasses. *Journal of molecular structure* 963, 82-86.
- [4] Yang, J., Dai, S., Dai, N., Xu, S., Wen, L., Hu, L. and Jing, Z. (2003). Effect of Bi_2O_3 on the spectroscopic properties of erbium-doped bismuth silicate glasses. *J. Opt. Soc. Am. B* 20, 810
- [5] Simon, S. and Todea, M. (2006). Spectroscopic study on iron silica-bismuth glasses and glass ceramics. *J. Non-Cryst. Solids* 352, 2947.
- [6] Beganskiene, A., Sirutkaitis, V., Kurtinaitiene, M., Juskenas, R. and Kareiva, A. (2004). FTIR, TEM, NMR, Investigation of Stober Silica Nanoparticles. *Materials Science* 10, 287.
- [7] Aruna, V., Sooraj Hussain N, Buddhudu, S. (1998). Spectra of Sm^{3+} and $\text{Dy}^{3+}:\text{B}_2\text{O}_3\text{-P}_2\text{O}_5\text{-R}_2\text{SO}_4$ Glasses. *Mater. Res. Bull.* 33: 149-59
- [8] Sooraj Hussain, N., Aruna, V. and Buddhudu, S. (2000), Absorption and Photoluminescence spectra of $\text{Sm}^{3+}:\text{TeO}_2\text{-B}_2\text{O}_3\text{-P}_2\text{O}_5\text{-Li}_2\text{O}$ glass of *Mater. Res. Bull.* 35:703-709.
- [9] Tanabe, S., Kang, J., Hanada, T. and Soga, N. (1998). Spectroscopic properties and Judd-Ofelt theory analysis of Dy^{3+} doped oxyfluoride silicate glass *Journal of Non-Crystal Solids* 239, 170.
- [10] Yu, M., Lin, J., Wang, J., Fu, J., Wang, S., Zhang, H.J. and Han, Y.C. (2002). Fabrication, patterning, and optical properties of nanocrystalline $\text{YVO}_4:\text{A}$ (A = Eu^{3+} , Dy^{3+} , Sm^{3+} , Er^{3+}) phosphor films via sol-gel soft lithography *Chem. Mater.* 14, 2224.
- [11] Lakshminarayana, G., Qiu, J. (2009). Photoluminescence of Pr^{3+} , Sm^{3+} and Dy^{3+} -doped $\text{SiO}_2\text{-Al}_2\text{O}_3\text{-BaF}_2\text{-GdF}_3$ glasses. *Journal of Alloys and Compounds.* 476, 70.
- [12] Rajesh, D., Balakrishna, A. and Ratnakaram, Y.C. (2012). Luminescence, structural and dielectric properties of Sm^{3+} impurities in strontium lithium bismuth borate glasses. *Opt. Mat.* 35, 108-116.
- [13] Pal, I., Agarwal, S. and Aggarwal, M.P. (2012). Structure and optical absorption of Sm^{3+} and Nd^{3+} ions in cadmium bismuth borate glasses with large radiative transition probabilities, *Opt. Mater.* 34, 1171-1180.b
- [14] Gorller-Walrand, C. and Binnemans, K. (1988). Spectral Intensities of f-f Transition. In: Gshneidner Jr., K.A. and Eyring, L., Eds., *Handbook on the Physics and Chemistry of Rare Earths*, Vol. 25, Chap. 167, North-Holland, Amsterdam, 101.



- [15] Sharma, Y.K., Surana, S.S.L. and Singh, R.K. (2009) Spectroscopic Investigations and Luminescence Spectra of Sm³⁺ Doped Soda Lime Silicate Glasses. *Journal of Rare Earths*, 27, 773.
- [16] Judd, B.R. (1962). Optical Absorption Intensities of Rare Earth Ions. *Physical Review*, 127, 750.
- [17] Ofelt, G.S. (1962) Intensities of Crystal Spectra of Rare Earth Ions. *The Journal of Chemical Physics*, 37, 511.
- [18] Sinha, S.P. (1983). Systematics and properties of lanthanides, Reidel, Dordrecht.
- [19] Krupke, W.F. (1974). *IEEE J. Quantum Electron* QE, 10, 450.
- [20] Meena, S.L. (2017). Spectroscopic Properties of Sm³⁺ Doped in Zinc Lithium Bismuth Borate Glasses. *Int. Journal of pure and applied physics*, 13, 485-494.
- [21] Meena, S.L. (2017). Spectroscopic Properties of Sm³⁺ Doped in Yttrium Zinc Lithium Bismuth Borate Glasses. *Journal of pure applied and Ind. physics*, 7, 1-9.

Table 5: Emission peak wave lengths (λ_p), radiative transition probability (A_{rad}), branching ratio (β), stimulated emission cross-section (σ_p) and radiative life time (τ_R) for various transitions in Sm^{3+} doped LLBS (SM) glasses.

Transition	λ_{max} (nm)	LLBS SM (01)				LLBS SM (1.5)				LLBS (SM 02)			
		$A_{rad}(s^{-1})$	β	σ_p ($10^{-20} cm^2$)	$\tau_R(\mu s)$	$A_{rad}(s^{-1})$	β	σ ($10^{-20} cm^2$)	$\tau_R(\mu s)$	$A_{rad}(s^{-1})$	β	σ_p ($10^{-20} cm^2$)	$\tau(\mu s)$
$^4G_{5/2} \rightarrow ^6H_{5/2}$	562	13.193	0.0409	0.0044	3098.22	13.300	0.0427	0.0049	3102.70	13.277	0.0413	0.0052	3108.68
$^4G_{5/2} \rightarrow ^6H_{7/2}$	600	141.860	0.4395	0.0477		141.857	0.4401	0.0512		141.941	0.4412	0.0565	
$^4G_{5/2} \rightarrow ^6H_{9/2}$	646	133.225	0.4128	0.0462		132.566	0.4113	0.0482		131.891	0.4100	0.0498	
$^4G_{5/2} \rightarrow ^6H_{11/2}$	705	34.487	0.1068	0.0138		34.574	0.1073	0.0146		34.571	0.1074	0.0151	